Theory and Practice of Enzyme Bioaffinity Electrodes. Chemical, Enzymatic, and Electrochemical Amplification of in Situ Product Detection

ARTICLE *in* JOURNAL OF THE AMERICAN CHEMICAL SOCIETY · JULY 2008

Impact Factor: 12.11 · DOI: 10.1021/ja7102873 · Source: PubMed

4 AUTHORS, INCLUDING:

Benoît Limoges
Paris Diderot University
118 PUBLICATIONS **2,318** CITATIONS
SEE PROFILE

Damien Marchal
Paris Diderot University
36 PUBLICATIONS **456** CITATIONS
SEE PROFILE

François Mavré
Paris Diderot University
34 PUBLICATIONS **602** CITATIONS
SEE PROFILE

J|A|C|S
ARTICLES

Published on Web 05/20/2008

Theory and Practice of Enzyme Bioaffinity Electrodes. Chemical, Enzymatic, and Electrochemical Amplification of in Situ Product Detection

Benoît Limoges,* Damien Marchal, François Mavré, and Jean-Michel Savéant*

Laboratoire d'Electrochimie Moléculaire, Université Paris Diderot, UMR CNRS 7591, 2 place Jussieu, 75251 Paris Cedex 05, France

Received November 22, 2007; E-mail: limoges@univ-paris-diderot.fr; saveant@univ-paris-diderot.fr

Abstract: The two articles in this series are dedicated to bioaffinity electrodes with in situ detection of the product of the enzyme label after recognition by its conjugate immobilized on the electrode. Part 1 was devoted to direct electrochemical detection, whereas the present contribution deals with homogeneous chemical and enzymatic amplification of the primary electrochemical signal. The theoretical relationships that are established for these modes of amplification are applied to the avidin–biotin recognition in a system that involves alkaline phosphatase as enzyme label and 4-amino-2,6-dichloro-phenyl phosphate as substrate, generating 2,6-dichloro-4-aminophenol as electrochemically active product. Chemical amplification then results from the addition of NADH, which reduces the 2,6-dichloro-quinonimine resulting from the electrochemical oxidation of 2,6-dichloro-4-aminophenol. An increased amplification is obtained when the reduction of 2,6-dichloro-quinonimine involves diaphorase in solution with NADH as substrate. The excellent agreement between theoretical predictions and experimental data required a detailed theoretical analysis and the independent determination of the key kinetic parameters of the system. The theoretical analysis was extended to monolayer and multilayered films of auxiliary enzyme as well as to electrochemical amplification by means of closely spaced dual electrodes so as to offer a rational comparative panorama of the amplification capabilities of the various possible strategies. Confinement of the profile of the product, and/or its oxidized form, in the vicinity the electrode surface appears as a key parameter of amplification.

Introduction

As discussed in details in the introduction of Part 1[1] of this series, enzyme-amplified binding assays associated with electrochemical detection have progressively emerged over the last fifteen years as a viable and attractive alternative to optical methods. There are two main ways of transducing the activity of the enzyme label immobilized on the electrode into an electrochemical signal. One in which the current is the electrocatalytic response of a redox couple serving as cosubstrate to a redox enzyme label and the other where transduction consists in the electrochemical detection of the enzyme label product.

Concerning the latter approach, the theoretical relationships characterizing the direct electrochemical detection of the enzyme label product in conventional high volume-to-surface cells have been established and tested experimentally in Part 1. It has also been shown, on theoretical and experimental grounds, that the sensitivity can be significantly improved by use of electrochemical cells with small volume-to-surface ratios. Another possibility consists in increasing the response of the enzyme label product by redox cycling.[2] This is feasible when the enzyme-generated product is a redox compound that can be reversibly oxidized or reduced. Among the numerous approaches that have been proposed, one-step in situ strategies are particularly attractive in terms of simplicity and efficiency when applied to bioaffinity electrodes. The bioaffinity electrode serves both as an immobilization platform of the binding recognition, allowing to specifically attaching the enzyme label onto the electrode surface, and as an electrochemical detector. These one-step in situ strategies consist in a continuous regeneration of the enzyme label product as production goes along in the close vicinity of the bioaffinity electrode. The electrochemical redox cycling between two working electrodes held at different potentials to cause alternative oxidation and reduction of the redox product generated by the enzyme label has been the most widely investigated in this respect.[3–10] The electrochemical cycling is efficient if the two electrodes are very close to each other as in

(1) Limoges, B.; Mavré, F.; Marchal, D.; Savéant,J.-M.; Schöllhorn, B. *J. Am. Chem. Soc.* **2008**, *130*, 7259–7275.
(2) Scheller, F. W.; Bauer, C. G.; Makower, A.; Wollenberger, U.; Warsinke, A.; Bier, F. F. *Anal. Lett.* **2001**, *34*, 1233–12.
(3) Niwa, O.; Xu, Y.; Halsall, H. B.; Heineman, W. R. *Anal. Chem.* **1993**, *65*, 1559–63.
(4) Thomas, J. H.; Kim, S. K.; Hesketh, P. J.; Halsall, H. B.; Heineman, W. R. *Anal. Biochem.* **2004**, *328*, 113–22.
(5) Thomas, J. H.; Kim, S. K.; Hesketh, P. J.; Halsall, H. B.; Heineman, W. R. *Anal. Chem.* **2004**, *76*, 2700–7.
(6) Kim, S. K.; Hesketh, P. J.; Li, C.; Thomas, J. H.; Halsall, H. B.; Heineman, W. R. *Biosens. Bioelectron.* **2004**, *20*, 887–94.
(7) Nebling, E.; Grunwald, T.; Albers, J.; Schäfer, P.; Hintsche, R. *Anal. Chem.* **2004**, *76*, 689–96.
(8) Gabig-Ciminska, M.; Holmgren, A.; Andresen, H.; Bundvig Barken, K.; Wumpelmann, M.; Albers, J.; Hintsche, R.; Breitenstein, A.; Neubauer, P.; Los, M.; Czyz, A.; Wegrzyn, G.; Silfversparre, G.; Jurgen, B.; Schweder, T.; Enfors, S.-O. *Biosens. Bioelectron.* **2004**, *19*, 537–46.
(9) Liu, D.; Perdue, R. K.; Sun, L.; Crooks, R. M. *Langmuir* **2004**, *20*, 5905–10.

10.1021/ja7102873 CCC: $40.75

Scheme 1. Various Modes of Redox Cycling Amplification

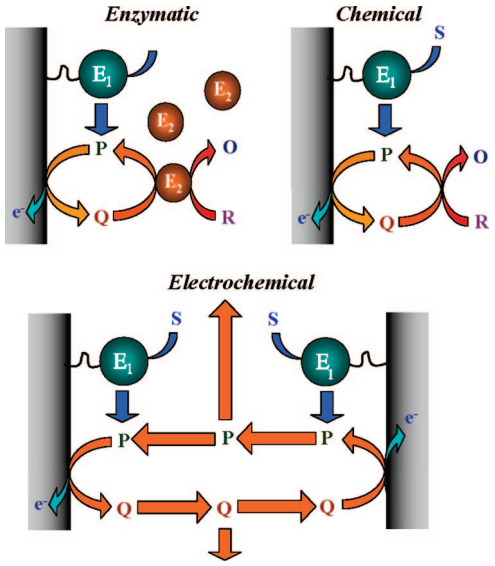

interdigitated electrode arrays.[3–10] However, these microdevices are difficult to fabricate and fragile. It should also be noted that the lack of theoretical analysis of these systems has so far prevented a rational evaluation of their performances.

Enzymatic amplification of the electrochemical signal of the enzyme label product seems a promising strategy in terms of simplicity and sensitivity. Although multienzymatic systems have attracted active attention,[11–17] it is only recently that enzymatic catalytic amplification has been specifically applied to one-step in situ amplification of the signal of enzyme bioaffinity electrodes.[18] Amplification factors higher than 3000 could thus be reached by co-immobilization with the first enzyme of a monolayer of an appropriate enzyme amplifier.

In the same vein, signal amplification by means of chemical regeneration has been recently proposed.[19] The method consists in the electrochemical oxidation of the reduced form of the enzyme label product and its regeneration by means of a chemical reagent added to the solution (Scheme 1).

Although the high amplification rates achieved with the immobilized bienzymatic system are quite attractive for developing highly sensitive biological assays,[18] co-immobilization of the two enzymes on the electrode surface complicates the procedure. The approach that consists in adding the enzymatic amplifier in the solution (Scheme 1) is more practicable. It has

Scheme 2

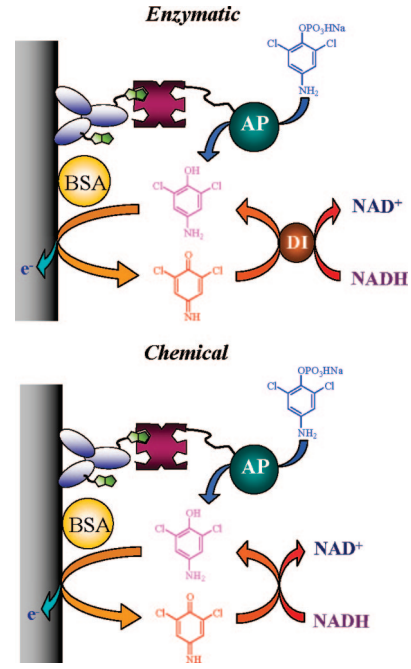

however never been investigated to the best of our knowledge. The main objective of the present work was thus to examine the potentiality of this approach and to compare it with the alternative strategy of chemical regeneration. As in Part 1 of the series, attainment of this goal requires the establishment of the theoretical relationships that link the electrochemical current response to the amount of primary enzyme label specifically attached to the electrode surface and therefore determine the key parameters that govern signal amplification in the enzymatic and in the chemical case. To complete the comparison, we have also derived the relationships pertaining to electrochemical amplification in conditions that mimic those where oppositely polarized close-spaced electrodes are used (Scheme 1).

To illustrate the applicability of the theoretical relationships thus derived to an experimental system and evaluate the amplification achievements of the various approaches, we have selected alkaline phosphatase (AP) as primary enzyme label. It is able to rapidly hydrolyze the substrate 4-amino-2,6-dichlorophenyl phosphate (2,6-DCPAPP) into an electroactive redox compound, the 4-amino-2,6-dichlorophenol (2,6-DCPAP), by a reversible two-electrons/two-proton exchange at the electrode.[1] The substrate/product couple 2,6-DCPAPP/2,6-DCPAP was preferred to the classical *p*-aminophenylphosphate/*p*-aminophenol couple because 2,6-DCPAP has a faster apparent heterogeneous electron transfer rate at an electrode coated with proteins than *p*-aminophenol.[1] This better-defined reversibility indeed improves the redox regeneration efficiency. As enzyme amplifier, we have chosen the diaphorase (DI) from *Bacillus stearothermophilus*, a redox enzyme that we previously characterized kinetically.[20] Assembling AP-based bioaffinity electrode with DI regeneration was as depicted in Scheme 2, showing the specific binding of alkaline phosphatase-conjugated neutravidin (N-AP) to a monolayer of biotinylated immunoglobulin (b-IgG) irreversibly adsorbed on the surface of a glassy carbon electrode, followed by the amplified electrochemical

(10) Honda, N.; Inaba, M.; Katagiri, T.; Shoji, S.; Sato, H.; Homma, T.; Osaka, T.; Saito, M.; Mizuno, J.; Wada, Y. *Biosens. Bioelectron.* **2005**, *20*, 2306–9.
(11) Yamaguchi, S.; Ozawa, S.; Ikeda, T.; Senda, M. *Anal. Sci.* **1992**, *8*, 87–8.
(12) Della Ciana, L.; Bernacca, G.; Bordin, F.; Fenu, S.; Garetto, F. *J. Electroanal. Chem.* **1995**, *381*, 129–35.
(13) Ito, S.; Yamazaki, S.; Kano, K.; Ikeda, T. *Anal. Chim. Acta* **2000**, *424*, 57–63.
(14) Rose, A.; Nistor, C.; Emnéus, J.; Pfeiffer, D.; Wollenberger, U. *Biosens. Bioelectron.* **2002**, *17*, 1033–43.
(15) Nistor, C.; Rose, A.; Wollenberger, U.; Pfeiffer, D.; Emneus, J. *Analyst* **2002**, *127*, 1076–81.
(16) Cardosi, M. F.; Birch, S. W.; Stanley, C. J.; Johannsson, A.; Turner, A. P. F. *Am. Biotech. Lab.* **1989**, *7*, 50–8.
(17) Bauer, C. G.; Eremenko, A. V.; Ehrentreich-Förster, E.; Bier, F. F.; Makower, A.; Halsall, H. B.; Heineman, W. R.; Scheller, F. W. *Anal. Chem.* **1996**, *68*, 2453–8.
(18) Limoges, B.; Marchal, D.; Mavré, F.; Savéant, J.-M. *J. Am. Chem. Soc.* **2006**, *128*, 6014–5.
(19) Das, J.; Jo, K.; Lee, J. L.; Yang, H, *Anal. Chem.* **2007**, *79*, 2790–6.
(20) Limoges, B.; Marchal, D.; Mavré, F.; Savéant, J.-M. *J. Am. Chem. Soc.* **2006**, *128*, 2084–92.

Scheme 3

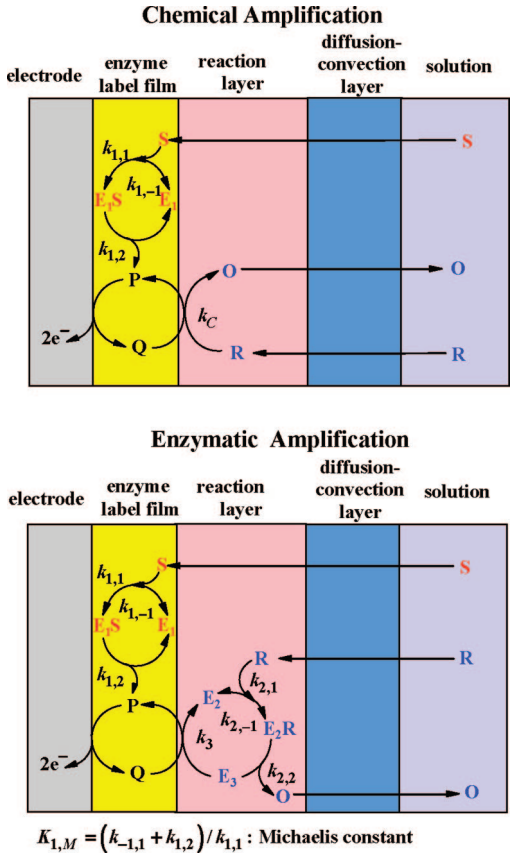

detection of the activity of the AP label in the presence of DI. Once the 2,6-DCPAP is generated by AP it is immediately oxidized at the electrode into 2,6-dichloro-quinonimine (2,6-DCQI) according to a $-2e^- - 2H^+$ reaction. In the presence of the auxiliary enzyme DI, the 2,6-DCQI is reduced back to 2,6-DCPAP and the oxidized form of DI is finally regenerated in its reduced native state by its natural substrate, NADH.

Selection of this bienzymatic system was guided by the fact that DI has a very high reactivity toward quinonimine derivatives, with a bimolecular rate constant close to diffusion control (i.e., higher than 10^8 M^{-1} s^{-1}), and also because both enzymes have their optimal activity within the same pH range (~8.5 for DI and ~9.5 for AP).

As a chemical amplification example, we chose the same system with no DI present. 2,6-DCPAP is then chemically regenerated by direct reduction of 2,6-DCQI by NADH in the solution.

Results and Discussion

1. Theoretical Relationships for Steady-State Chronoamperometry and Cyclic Voltammetry. 1.1. General. The primary enzyme E_1 is assumed to follow a simple Michaelis–Menten kinetics (involving two forms, E_1 and E_1S), while the secondary enzyme, serving as amplifier, is considered to operate according to a classical ping-pong mechanism (involving the three forms E_2, E_2,R and E_3). For the chemical regeneration a simple irreversible bimolecular reaction is considered. Scheme 3 shows the various layers that are met successively when going toward the solution perpendicularly to the electrode surface (assumed to be planar). The familiar enzyme label film and the diffusion-natural convection layer,[1] are enfolding the "reaction layer" in which the chemical or enzymatic regenerating reaction takes place. Since the chemical or enzymatic reactions of interest are fast, the reaction layer is thin, much thinner than the diffusion-convection layer (unlike what is represented in Scheme 3). As soon as the enzyme bioaffinity electrode is immersed in a solution containing the substrate S, P is produced at the electrode surface, diffuses in the solution, and is oxidized into Q if the electrode potential is set at an appropriate value (we consider oxidations, but what follows is easily transposed to reductions). Taking into account that the primary enzyme film is much thinner than the diffusion and diffusion-reaction layers in the solution, the resulting flux balance writes

$$\frac{I}{2F} = D\left(\frac{\mathrm{d}[P]}{\mathrm{d}x}\right)_{x=0} + k_{1,2}\Gamma_{E_1S} = -D\left(\frac{\mathrm{d}[Q]}{\mathrm{d}x}\right)_{x=0} \qquad (1)$$

where I is the current density. Here and below, D is the diffusion coefficient of P and Q and is assumed to be approximately the same, the square brackets represent the corresponding concentrations, and Γ is the surface concentrations of the subscript forms of enzyme. The subscript $x = 0$, indicates that the fluxes and concentrations are taken at the electrode or at the enzyme layer surfaces in the framework of linear diffusion. The two corresponding average planes may be confounded since the thickness of the enzyme film is small as compared to the diffusion layer (the thicknesses in Scheme 3 are arbitrary). The factor 2 in the first member of the above equation is a stoichiometric factor expressing the fact that the electrochemical oxidation of the product consumes two electrons per molecule as in the illustrating example below and as in a number of other cases. In the framework of Michaelis–Menten kinetics, the steady-state enzymatic production of P, to be introduced in eq 1, may be expressed as

$$k_{1,2}\Gamma_{E_1S} = k_{1,2}\Gamma^0_{E_1}\frac{[S]_{x=0}}{K_{M,1} + [S]_{x=0}}$$

where $\Gamma^0_{E_1}$ is the surface concentration of the enzyme labeled recognized analyte. In the general case, when both the enzyme kinetics and substrate diffusion jointly govern the production of P (see Part 1):

$$k_{1,2}\Gamma_{E_1S} = \frac{D_S C^0_S}{\delta} \times \frac{1 + \frac{K_{1,M}}{C^0_S} + \frac{k_{1,2}\Gamma^0_{E_1}\delta}{D_S C^0_S} - \sqrt{\left(1 + \frac{K_{1,M}}{C^0_S} + \frac{k_{1,2}\Gamma^0_{E_1}\delta}{D_S C^0_S}\right)^2 - 4\frac{k_{1,2}\Gamma^0_{E_1}\delta}{D_S C^0_S}}}{2} \qquad (2)$$

(D_S is the diffusion coefficient of S and C^0_S, its bulk concentration, δ is the diffusion-natural convection layer thickness). This expression simplifies to

$$k_{1,2}\Gamma_{E_1S} = k_{1,2}\Gamma^0_{E_1} \qquad (3)$$

when the bulk substrate concentration is increased so as to reach a situation where the production of P is solely governed by a saturated Michaelis–Menten kinetics with no interference of substrate diffusion.

1.2. Chemical Amplification. P linearly diffuses in the portion of space adjacent to the electrode and to the enzyme label surface, while being regenerated by solution reduction of Q that

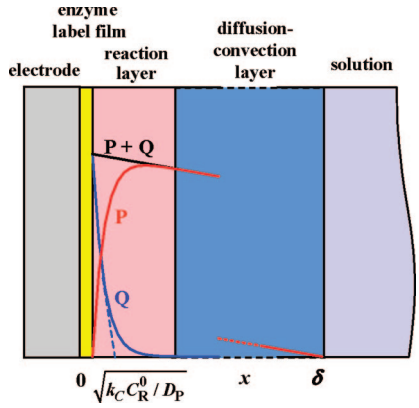

Figure 1. Chemical amplification. Concentration profiles.

has been produced by the oxidation of P at the electrode. These combined events are governed by the following equations.

$$D\frac{d^2[P]}{dx^2} + k_C C_R^0[Q] = 0 \quad (4)$$

$$D\frac{d^2[Q]}{dx^2} - k_C C_R^0[Q] = 0 \quad (5)$$

The neglect of the variations of [P] and [Q] with time follows from the fact that regenerating reactions of interest are fast, so fast that a steady state is reached resulting from the mutual compensation of diffusion and chemical reaction. These "pure kinetic conditions"[21] also entail the confinement of the Q profile within a thin layer, the "reaction layer", adjacent to the electrode surface. Moreover, in writing eqs 4 and 5, we have considered the case where the concentration of the substrate R is large enough for being constant throughout the reaction layer and equal to its bulk concentration, C_R^0. Under these conditions, the current response in cyclic voltammetry and chronoamperometry can be obtained as follows. Addition of eqs 4 and 5, followed by integration leads to (see Figure 1):

$$[P] + [Q] = \frac{k_{1,2}\Gamma_{E_1S}}{D}(\delta - x) \quad (6)$$

after having taken into account eq 1 and $[P]_{x=\delta} + [Q]_{x=\delta} = 0$ as boundary conditions at $x=0$ and $x = \delta$, respectively.

Integration of eq 5 alone taking into account the "pure kinetic conditions" leads to

$$\frac{I}{2F} = -D\left(\frac{d[Q]}{dx}\right)_{x=0} = \sqrt{Dk_C C_R^0}[Q]_{x=0}$$

From eq 6:

$$[P]_{x=0} + [Q]_{x=0} = \frac{k_{1,2}\Gamma_{E_1S}\delta}{D}$$

If the electrode potential is positive enough for the condition to be fulfilled $[P]_{x=0} = 0$, then

$$[Q]_{x=0} = \frac{k_{1,2}\Gamma_{E_1S}\delta}{D} \quad (7)$$

and therefore

$$\frac{I}{2F} = \sqrt{\frac{k_C C_R^0}{D}}\delta k_{1,2}\Gamma_{E_1S} \quad (8)$$

This steady state current is the one observed in chronoamperometry when the electrode potential is poised at a sufficiently positive potential. It would be reached along an S-shaped curve in cyclic voltammetry at the end of the scan. The final expression of the current is obtained from eq 8 after replacement of $\Gamma_{E_1}S$ by its expression in eq 2:

$$\frac{I}{2F} = \sqrt{\frac{k_C C_R^0}{D}}\delta\frac{D_S C_S^0}{\delta} \times \frac{1 + \frac{K_{1,M}}{C_S^0} + \frac{k_{1,2}\Gamma_{E_1}^0\delta}{D_S C_S^0} - \sqrt{\left(1 + \frac{K_{1,M}}{C_S^0} + \frac{k_{1,2}\Gamma_{E_1}^0\delta}{D_S C_S^0}\right)^2 - 4\frac{k_{1,2}\Gamma_{E_1}^0\delta}{D_S C_S^0}}}{2} \quad (9)$$

or, more simply by its expression in eq 3, when the substrate concentration is large enough for reaching saturated Michaelis–Menten kinetics. In the latter case,

$$\frac{I}{2F} = \sqrt{\frac{k_C C_R^0}{D}}\delta k_{1,2}\Gamma_{E_1}^0 \quad (10)$$

The P and Q concentration profiles in the reaction and diffusion layers, shown in Figure 1 are given by the following equation and by eq 7.

$$[Q] = \frac{k_{1,2}\Gamma_{E_1S}\delta}{D}\exp\left(-x\sqrt{\frac{k_C C_R^0}{D}}\right)$$

1.3. Enzymatic Amplification. The analysis is similar to the preceding case. The only change is the replacement of eqs 5 and 6 by the equations that describe the kinetics of the amplifying enzyme in the reaction layer:

$$D\frac{\partial^2[P]}{\partial x^2} + \frac{C_{E_2}^0}{\frac{1}{k_3[Q]} + \frac{1}{k_{2,2}} + \frac{1}{k_2 C_R^0}} = 0$$

$$D\frac{\partial^2[Q]}{\partial x^2} - \frac{C_{E_2}^0}{\frac{1}{k_3[Q]} + \frac{1}{k_{2,2}} + \frac{1}{k_2 C_R^0}} = 0 \quad (11)$$

with $k_2 = k_{2,2}/K_{2,M}$ and $K_{2,M} = (k_{2,-1} + k_{2,2})/k_{2,1}$.

Integration of eq 11 under "pure kinetic conditions" leads to

$$-\left(\frac{\partial[Q]}{\partial x}\right)_{x=0} = [Q]_{x=0}\sqrt{\frac{k_3 C_{E_2}^0}{D_P}}\sqrt{\frac{2}{k_3[Q]_{x=0}\left(\frac{1}{k_{2,2}} + \frac{1}{k_2 C_R^0}\right)}} \times \sqrt{1 - \frac{\ln\left(1 + k_3[Q]_{x=0}\left(\frac{1}{k_{2,2}} + \frac{1}{k_2 C_R^0}\right)\right)}{k_3[Q]_{x=0}\left(\frac{1}{k_{2,2}} + \frac{1}{k_2 C_R^0}\right)}}$$

by analogy with the derivations in ref 22. Maximizing the enzymatic amplification by using large concentrations of the substrate R pushes the enzymatic kinetics in the saturated Michaelis–Menten limit:

(21) Savéant, J.-M. *Elements of Molecular and Biomolecular Electrochemistry*; Wiley-Interscience: New York, 2006; Chapter 2.

(22) Limoges, B.; Moiroux, J.; Savéant, J.-M. *J. Electroanal. Chem.* **2002**, *521*, 1–7.

$$-\left(\frac{\partial[Q]}{\partial x}\right)_{x=0} = [Q]_{x=0}\sqrt{\frac{k_3 C^0_{E_2}}{D}}\sqrt{\frac{2}{\frac{k_3[Q]_{x=0}}{k_{2,2}}}}\sqrt{\left[1-\frac{\ln\left(1+\frac{k_3[Q]_{x=0}}{k_{2,2}}\right)}{\frac{k_3[Q]_{x=0}}{k_{2,2}}}\right]}$$

Taking the still valid eqs 1 and 7 into account, the cyclic voltammetric plateau current or chronoamperometric steady-state current may be expressed as

$$\frac{I}{2F} = k_{1,2}\Gamma_{E_1S}\delta\sqrt{\frac{k_3 C^0_{E_2}}{D}}\sqrt{\frac{2}{\frac{k_3 k_{1,2}\Gamma_{E_1S}\delta}{k_{2,2}D}}}\sqrt{\left[1-\frac{\ln\left(1+\frac{k_3 k_{1,2}\Gamma_{E_1S}\delta}{k_{2,2}D}\right)}{\frac{k_3 k_{1,2}\Gamma_{E_1S}\delta}{k_{2,2}D}}\right]} \quad (12)$$

The final expression of the limiting current density is obtained from eq 12 after replacement of Γ_{E_1S} by its expression in eq 2 or, more simply, by its expression in eq 3, when the substrate concentration is large enough for reaching saturated Michaelis–Menten kinetics. In the latter case, Γ_{E_1S} is simply replaced by $\Gamma^0_{E_1}$ in eq 12.

The main objective of amplification is the detection of small amount of the enzyme label on the electrode surface, that is, small values of $\Gamma^0_{E_1}$. Under these conditions eq 13 becomes simply

$$\frac{I}{2F} = k_{1,2}\Gamma_{E_1S}\delta\sqrt{\frac{k_3 C^0_{E_2}}{D}} \quad (13)$$

reflecting the fact that the production of P by the first enzyme being slow, the rate-determining constant in the kinetics of the second enzyme becomes k_3. Here again, Γ_{E_1S} may be replaced by $\Gamma^0_{E_1}$ when the substrate concentration is large enough for reaching saturated Michaelis–Menten kinetics. Then

$$\frac{I}{2F} = k_{1,2}\Gamma^0_{E_1}\delta\sqrt{\frac{k_3 C^0_{E_2}}{D}} \quad (14)$$

1.4. Electrochemical Amplification. In the electrode configuration sketched in the bottom figure of Scheme 1 that mimics an electrochemical redox cycling at parallel electrodes, amplification results from opposite polarization of the two electrodes. Amplification will be maximized if, for example, the left electrode is polarized at a potential sufficiently positive to enforce the condition [P] = 0 at its surface and the right electrode polarized at a potential sufficiently negative to enforce the condition [Q] = 0 at its surface. Then the Q generated at the left electrode diffuses in the interelectrode gap to the right electrode where it is reduced into P that diffuses back to the left electrode where it is oxidized and so on. A symmetrical succession of events takes place at the right electrode. In addition to these back-and-forth diffusions from one electrode to the other, P and Q tend to diffuse out of the interelectrode gap toward the bulk of the electrochemical cell. Since we do not need a very precise estimate of the mutual collection efficiency of the dual electrodes, we can transform the actual system into the equivalent simplified arrangement sketched in Scheme 4,

Scheme 4

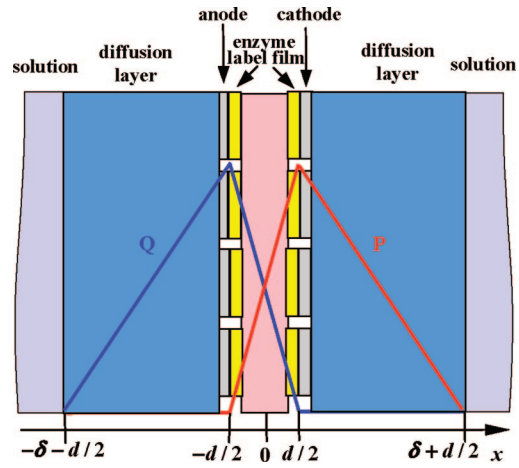

where formal holes are pierced through each electrode and its immobilized enzyme layer, so as to allow the diffusion of P and Q not only to the other electrode but also within an external steady-state diffusion layer of thickness δ. Under these conditions the balance of fluxes of P writes

$$\frac{I_c}{2F} + k_{1,2}\Gamma_{E_1S} = D\frac{[P]_{x=d/2}}{\delta} + D\frac{[P]_{x=d/2}}{d}$$

at the right electrode (cathode) and

$$-\frac{I_a}{2F} - k_{1,2}\Gamma_{E_1S} = D\frac{[P]_{x=d/2}}{d}$$

at the left electrode (anode). At steady-state, $I_c = -I_a = I$, and therefore

$$\frac{I}{2F} = k_{1,2}\Gamma_{E_1S}\left(1+2\frac{\delta}{d}\right) \simeq 2k_{1,2}\Gamma_{E_1S}\frac{\delta}{d}$$

(in practical applications $d \ll \delta$), in which Γ_{E_1S} should be replaced by its expression in eq 2 or, more simply, by $\Gamma^0_{E_1}$ when the substrate concentration is large enough for reaching saturated Michaelis–Menten kinetics.

1.5. Comparison of Amplification Rates. Confinement. We may define the amplification rate by reference to the steady-state chronoamperometric current, $I/2F = k_{1,2}\Gamma_{E_1S}$. In all three cases ampl $= \delta/\mu$, where μ is a distance characterizing each mode of amplification:

$$\text{chemical:} \quad \text{ampl} = \delta\sqrt{k_C C^0_R/D},\ \mu = \sqrt{D/k_C C^0_R} \quad (15)$$

$$\text{enzymatic:} \quad \text{ampl} = \delta\sqrt{k_3 C^0_{E_2}/D},\ \mu = \sqrt{D/k_3 C^0_{E_2}} \quad (16)$$

$$\text{electrochemical:} \quad \text{ampl} = 2\delta/d,\ \mu = d/2 \quad (17)$$

In the electrochemical case, the smallest value of $d/2$ is of the order of micrometers. Equivalent or smaller values of μ can be reached in the case of chemical and enzymatic amplification thanks to an appropriate choice of the amplifier and of its concentration as exemplified in the next section.

We thus see that amplification increases as a function of the increased confinement of the concentration profile of the oxidized substrate. The same notion also applies to the cyclic voltammetric sampling procedures detailed in Part 1. The confinement length is then the cyclic voltammetric diffusion layer $(RT/DFv)^{1/2}/A$, a decreasing function of the scan rate (A is the stoichiometric factor of the order of 0.7 defined in Part 1).

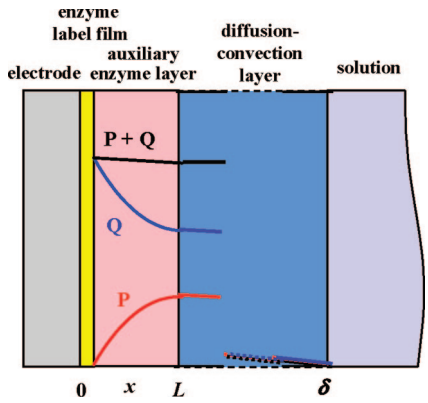

Figure 2. Enzymatic amplification with a multilayered immobilized enzyme film. Concentration profiles.

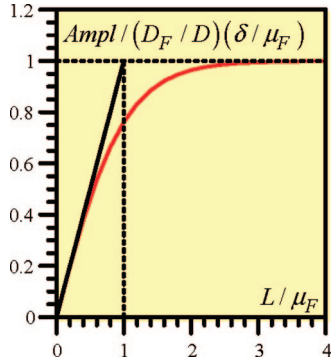

Figure 3. Enzymatic amplification with a multilayered immobilized enzyme film. Variation of the amplification rate with the film thickness.

It is also interesting to recall the equation giving the rate of enzymatic amplification when a monolayer of auxiliary enzyme is co-immobilized with the enzyme label on the electrode surface as described in a recent preliminary note,[18]

$$\text{ampl} = k_3\Gamma^0_{E_2}\delta/D \tag{18}$$

in conditions where k_3 is the rate-determining constant in the kinetics of the auxiliary enzyme. The corresponding "confinement length", $\mu = D/k_3\Gamma^0_{E_1}$, has no obvious physical meaning in this case. This notion gets back its relevance when examining the use of thicker, multilayered, auxiliary enzyme films. Their potential interest lies in an increase of the amplification rate as $\Gamma^0_{E_2}$ (intended as the total amount of enzyme per unit surface area) increases according to eq 18. However, the question arises of the validity of eq 18 as the film gets thicker and thicker. Indeed, as the thickness increases, a competition between the enzymatic reaction and diffusion of P and Q takes place inside the film. Figure 2 shows the various successive layers that are met upon going from the electrode to the solution. The enzymatic catalytic cycle that is running inside the light red zone designated as "auxiliary enzyme film" is the same as the one in the light red zone designated as "reaction layer" in Scheme 3.

Inside the film, that is, for $0 \le x \le L$:

$$D_F\frac{d^2[P]}{dx^2} + k_3C^0_{E_2}[Q] = 0 \tag{19}$$

$$D_F\frac{d^2[Q]}{dx^2} - k_3C^0_{E_2}[Q] = 0 \tag{20}$$

in conditions where k_3 is the rate-determining constant in the kinetics of the auxiliary enzyme, valid for low coverages of the enzyme label. D_F is the common value of the P and Q diffusion coefficients inside the film as opposed to D, their value in the solution. $C^0_{E_2} = \Gamma^0_{E_2}/L$ is the volume concentration of the auxiliary enzyme in the film and $\Gamma^0_{E_2}$ is the total amount of auxiliary enzyme per unit surface area. The boundary conditions at the electrode surface are embodied in the following expressions of the current density that derive from the flux balances for P and Q.

$$\frac{I}{2F} = k_{1,2}\Gamma_{E_1S} + D_F\left(\frac{d[P]}{dx}\right)_{x=0} = -D_F\left(\frac{d[Q]}{dx}\right)_{x=0}$$

$$[P]_{x=0} = 0$$

At the film/diffusion-convection layer interface:

$$-D_F\left(\frac{d[P]}{dx}\right)_{x=L_-} = -D\left(\frac{d[P]}{dx}\right)_{x=L_+} = D\frac{[P]_{x=L}}{\delta}$$

$$-D_F\left(\frac{d[Q]}{dx}\right)_{x=L_-} = -D\left(\frac{d[Q]}{dx}\right)_{x=L_+} = D\frac{[Q]_{x=L}}{\delta}$$

Introducing the reaction layer thickness,

$$\mu_F = \sqrt{\frac{D_F}{k_3C^0_{E_2}}} = \sqrt{\frac{LD_F}{k_3\Gamma^0_{E_2}}} \tag{21}$$

integration of eqs 19 and 20, taking the above boundary conditions into account, leads to

$$[Q] = k_{1,2}\Gamma_{E_1S}\frac{\delta}{D}\frac{\exp\left(\frac{x-L}{\mu_F}\right) + \exp\left(-\frac{x-L}{\mu_F}\right)}{\exp\left(\frac{L}{\mu_F}\right) + \exp\left(-\frac{L}{\mu_F}\right)}$$

Typical concentration profiles are shown in Figure 2 (for $L = \mu_F$). The current is given by

$$\frac{I}{2F} = k_{1,2}\Gamma_{E_1S}\frac{D_F}{D}\frac{\delta}{\mu_F}\tanh\left(\frac{L}{\mu_F}\right)$$

and thus:

$$\text{ampl} = \frac{D_F}{D}\frac{\delta}{\mu_F}\tanh\left(\frac{L}{\mu_F}\right) = \frac{D_F}{D}\delta\sqrt{\frac{k_3\Gamma^0_{E_2}}{LD_F}}\tanh\left(\sqrt{\frac{k_3\Gamma^0_{E_2}L}{D_F}}\right) \tag{22}$$

The variation of the amplification rate with the film thickness of auxiliary enzyme is represented in Figure 3. After an initial linear variation:

$$\text{ampl} \xrightarrow{\mu/L \to \infty} \frac{\delta}{D}k_3\Gamma^0_{E_2} = \frac{\delta}{D}k_3C^0_{E_2} \times L$$

where amplification increases proportionally to the thickness, or equivalently, to the total amount of enzyme per unit surface area; it tends asymptotically toward a limit:

$$\text{ampl} \xrightarrow{\mu/L \to 0} \frac{D_F}{D}\delta\sqrt{\frac{k_3\Gamma^0_{E_2}}{LD_F}} = \frac{D_F}{D}\delta\sqrt{\frac{k_3C^0_{E_2}}{D_F}}$$

After $L = \mu_F = (D_F/k_3C^0_{E_2})^{1/2}$, it is of no longer practical use to increase the film thickness. A typical example will be discussed in section 2.4.

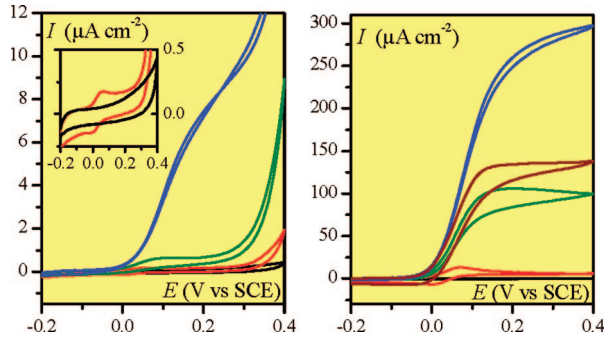

Figure 4. Cyclic voltammetric analysis of N-AP/b-IgG electrodes in a Tris buffer (pH = 9) at two coverages of b-IgG-N-AP prepared from a 10^{-12} M (left) and 10^{-10} M (right) N-AP solution, respectively: (black) Tris buffer alone; (red) 1 mM 2,6-DCPAPP; (green and brown)1 mM 2,6-DCPAPP + 4 mM NADH; (blue) 1 mM 2,6-DCPAPP + 4 mM NADH + 2 μM DI. Scan rate = 10 mV s^{-1} except for the brown and blue curves on the right where it is 200 mV s^{-1}. Insert shows magnified black and red curves.

2. Illustrating Example: Alkaline Phosphatase Amplified Avidin–Biotin Recognition Electrode with 4-Amino-2,6-dichloro-phenyl Phosphate as Substrate. 2.1. Chronoamperometric and Cyclic Voltammetric Responses with NADH as Chemical Amplifier and Diaphorase (with NADH as Substrate) as Enzymatic Amplifier. We investigated chemical amplification by taking advantage of the fact that NADH is known to be easily oxidized by a large variety of two-electrons-proton acceptors such as quinones and quinonimines.[23] NADH was also used as a substrate for diaphorase in our investigation of enzymatic amplification. The procedure was as follows. Once the b-IgG-coated electrode is loaded with the primary enzyme, N-AP (Scheme 2), and rinsed, it is immersed in an electrochemical cell containing 2,6-DCPAPP, the substrate of AP. Immediately after immersion, the N-AP specifically immobilized onto the electrode surface starts to convert the 2,6-DCPAPP into 2,6-DCPAP which diffuses in the solution. A steady-state diffusion-convection situation is established after a few seconds, giving rise to a reversible cyclic voltammogram, shown in red in Figure 4, located at 0.05 V versus SCE, which is characteristic of the reversible oxidation of the enzyme-generated 2,6-DCPAP.

The addition of NADH to the solution results in plateau-shaped cyclic voltammetric responses (green and brown curves in Figure 4) with a plateau current higher than the red curve peak as expected from a chemical amplification resulting from the regeneration of 2,6-DCPAP by reaction of NADH with 2,6-DCPQI. For highest N-AP surface concentration (right diagram) the voltammogram recorded at the lowest scan rate (0.01 V/s) is slightly peak-shaped as a result of partial consumption of the substrate (green curve). This phenomenon disappears upon raising the scan rate leading to a plateau-shaped curve (brown curve recorded at 0.2 V/s).

A plateau-shaped response with a significantly higher plateau current is observed (blue curves in Figure 4) upon further addition of DI to the preceding solution. The higher steady-state current demonstrates that regeneration of 2,6-DCPAP from 2,6-DCPQI in the presence of NADH is more efficient when the reaction is catalyzed by the enzyme diaphorase than by direct chemical reduction with NADH.

The same succession of events can be observed in steady-state chronoamperometry at a sufficiently positive potential to enforce the condition $[P]_{x=0} = 0$ as shown in Figure 5. The current decrease observed after the rise triggered by the addition of DI is the result of an excessive consumption of NADH in the reaction layer. This is confirmed by the fact that the decrease is much less after a further addition of NADH. The same phenomenon can be observed in cyclic voltammetry where it can be fought against by increasing the scan rate (Figure 4).

(23) Gorton, L., Domínguez, E. Electrochemistry of $NAD(P)^+$/NAD(P)H. In *Encyclopedia of Electrochemistry*; Wiley Interscience: Weinheim, Germany, 2002; Vol. 9, pp 67–144.

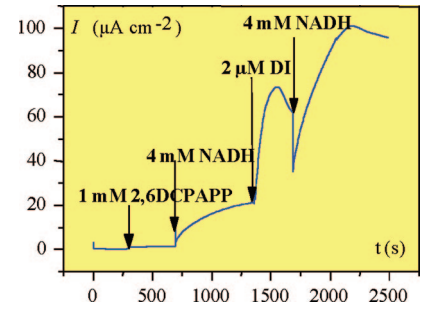

Figure 5. Chronoamperometric analysis of a N-AP/b-IgG electrode in a Tris buffer (pH = 9) prepared from a 5×10^{-11} M N-AP solution. Effect of the successive addition of 2,6-DCPAP, NADH, and DI is symbolized by the vertical arrows.

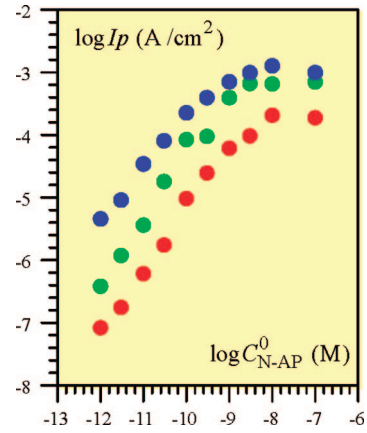

Figure 6. Calibration curves showing the variation of the voltammetric peak or plateau current density at a N-AP/b-IgG-modified electrode as a function of the N-AP concentration in which the bioaffinity electrode was initially incubated. The measurements were carried out in Tris buffer (pH = 9) containing 1 mM of 2,6-DCPAPP (red dots), 1 mM 2,6-DCPAPP + 4 mM NADH (green dots), or 1 mM 2,6-DCPAPP + 4 mM NADH + 2 μM DI (blue dots). $v = 10$ mV s^{-1}.

Systematic experiments of the type shown in Figure 4 were carried out for a range of concentrations of enzyme label in solution, $C^0_{N\text{-}AP}$, allowing one to obtain a series of b-IgG-N-AP electrodes with various enzyme label coverages. The resulting calibration curves relating the peak or plateau currents to $C^0_{N\text{-}AP}$ are shown in Figure 6.

Comparison between the theoretical predictions and these experimental results is carried out in section 2.3. It requires the prior determination of the rate parameters of the chemical and enzymatic amplifiers, which is the object of the next section.

2.2. Determination of the Rate Parameters of the Chemical and Enzymatic Amplifiers. Application of the relationships developed in section 1 to the above results requires the independent determination of the kinetic constants characterizing the chemical and enzymatic catalysis on which these two modes of amplification are based. These constants were derived from cyclic voltammetric experiments in which the reversible response of 2,6-DCPAPP is converted into a plateau-shaped curve

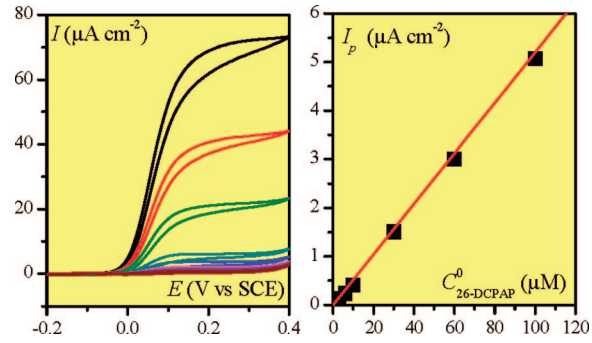

Figure 7. (Left) Cyclic voltammograms recorded at a glassy carbon electrode in a 0.1 M Tris buffer (pH = 9.0) containing 1 mM $MgCl_2$, 4 mM NADH and, from bottom to top, 0, 1, 2, 3, 6, 10, 30, 60, 100 μM 2,6-DCPAP. Scan rate = 0.03 V s^{-1}. (Right) Variation of the catalytic plateau current with the concentration of 2,6-DCPAP: (red solid line) fitting of data with eq 23 with $k_C = 900$ M^{-1} s^{-1}, $D_{2,6\text{-DCPAP}} = 4 \times 10^{-6}$ cm^2 s^{-1}.

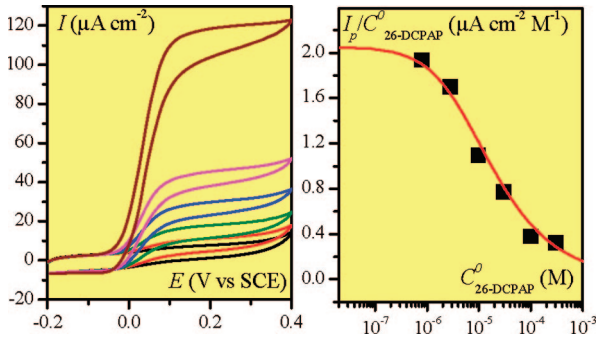

Figure 8. (Left) Cyclic voltammograms recorded at a GC electrode in a Tris buffer solution in presence of 4 mM NADH, 100 nM DI, and, from bottom to top, [2,6-DCPAP] = 0.8, 2.8, 9.8, 29.8, 100, 300 μM. (Right) Variation with 2,6-DCPAP concentration of the catalytic plateau current: (red line) best fit considering a bimolecular rate constant toward cosubstrate $k_3 = 3 \times 10^8$ M^{-1} s^{-1} and a turnover $k_{cat} = 1000$ s^{-1}. Scan rate = 0.1 V s^{-1}.

upon addition of NADH (Figure 7) and NADH + DI (Figure 8), respectively.

As expected, the plateau current is proportional to the concentration of 2,6-DCPAP, $C^0_{2,6\text{-DCPAP}}$ (Figure 7), and the square root of NADH concentration, C^0_{NADH} (not shown) according to[21,24]

$$I_p = 2FC^0_{2,6-DCPAP}\sqrt{D_{2,6-DCPAP}}\sqrt{k_C C^0_{NADH}} \qquad (23)$$

thus leading from fitting of the experimental data with eq 23 to $k_C = 900$ M^{-1} s^{-1}. Significantly higher plateau currents are obtained upon addition of a modest amount of DI (Figure 8). From the analysis of the variation of the plateau currents with the cosubstrate concentration, under saturated Michaelis–Menten conditions, one obtains $k_3 = 3 \times 10^8$ M^{-1} s^{-1} and $k_{2,2} = 1000$ s^{-1} according to the procedure described in ref 20.

2.3. Application of the Theoretical Relationships. Two additional pieces of information were required to analyze, according to the theoretical relationships developed in section 1, the results displayed in Figure 6 which summarizes all the data we have gathered using direct detection as well as chemical and enzymatic amplification. The first piece of information was the rate constants of N-AP attached to the b-IgG-coated electrode.

(24) Savéant, J-M.; Vianello, E. in *Advances in Polarography*; Longmuir, I., Ed.; Pergamon Press: New York, 1960; p 367.

Table 1. Parameters for the Analysis of the Experimental Data

δ (cm)	0.019
$D_P \approx D_S$ (cm^2 s^{-1})	4×10^{-6}
$k_{1,2}$ (s^{-1})	1500
$K_{1,M}$ (M)	5×10^{-5}
$\Gamma^0_{E_1,max}$ (mol cm^{-2})	1.5×10^{-12}
K_b (M^{-1})	7×10^7
k_C (M^{-1} s^{-1})	900
k_3 (M^{-1} s^{-1})	3×10^8
$k_{2,2}$ (s^{-1})	1000
C^0_S (M)	10^{-3}
C^0_R (M)	4×10^{-3}
$C^0_{E_2}$ (M)	2×10^{-6}

It was found to be approximately the same as in homogeneous solution (i.e., $k_{1,2} = 1500$ s^{-1}, $K_{1,M} = 50$ μM).[1] The second piece of information relates to the recognition isotherm assumed to be of the Langmuir type (see the first companion paper):

$$\Gamma^0_{E_1} = \Gamma^0_{E_1,max}\frac{K_b C^0_{N\text{-}AP}}{1 + K_b C^0_{N\text{-}AP}} \qquad (24)$$

with $K_b = 7 \times 10^7$ M^{-1} and $\Gamma^0_{E_1,max} = 1.5 \times 10^{-12}$ mol cm^{-2}.[1]

For convenience, the various constants required for the analysis of the experimental data are all gathered in Table 1.

The cyclic voltammetric data in Figure 6 (red dots) shows a linear variation at low values of $C^0_{N\text{-}AP}$, which corresponds to the linear (Henry) part of the Langmuir isotherm, while the leveling off observed upon increasing does not correspond to the saturated part of the Langmuir isotherm but rather to the fact that diffusion of the substrate, here 2,6-DCPAPP, becomes rate-limiting. Such behaviors have been analyzed in details in Part 1. We focus here on the variations exhibited under chemical and enzymatic amplification (Figure 9).

Considering first chemical amplification, we observe that at low values of $C^0_{N\text{-}AP}$, the plateau current adheres to the linear (Henry) part of the Langmuir isotherm. The leveling off at high values of $C^0_{N\text{-}AP}$ does not embody reaching saturation of the Langmuir isotherm (represented by the theoretical green dotted line in Figure 9). It rather indicates that the kinetic control of the enzyme label is passing from the enzymatic reaction to the

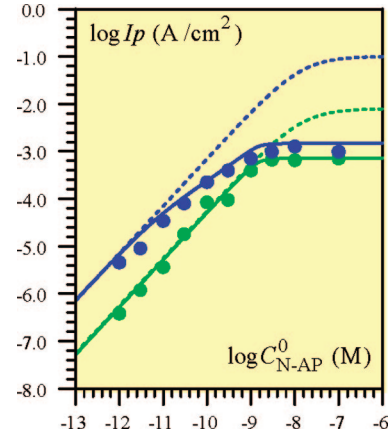

Figure 9. Calibration curves showing the variation of the voltammetric plateau current density at a N-AP/b-IgG-modified electrode with the N-AP concentration in the solution where the bioaffinity electrode was initially incubated for chemical (green dots) and enzymatic (blue dots) amplification under the same conditions as in Figure 6. Full and dotted green lines show the simulation according to 9 and 10, respectively. Full and dotted blue lines show the simulation according to eqs 12 and 2 and eq 14, respectively, taking additionally into account the chemical catalysis by NADH.

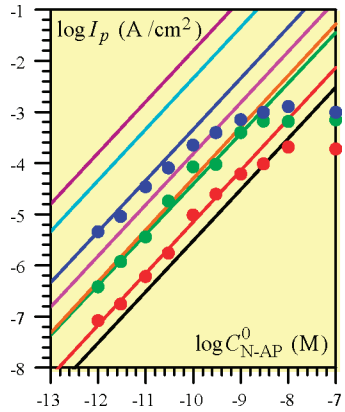

Figure 10. Calibration curves of the N-AP/b-IgG bioaffinity electrode in the same conditions as in Figures 6 and 9 obtained or expected for the following strategies: (black) nonamplified steady-state chronoamperometry; (red and brown) cyclic voltammetry at 0.01 and 0.5 V/s, respectively; (green) chemical amplification by NADH; (blue) enzymatic amplification by 2 μM DI in solution (and NADH as substrate); (magenta) dual electrode separated by 4 μm; (cyan) co-immobilized monolayer containing 1.5 pmol/cm^2 of auxiliary enzyme; (purple) co-immobilized four-monolayer containing each 1.5 pmol/cm^2 of auxiliary enzyme.

Table 2. Amplification Rates (ampl) and Confinement Lengths (μ)

amplification method		ampl	μ (μm)
steady-state chronoamperometry		1	190
cyclic voltammetry	v = 0.01 V/s	3	70
	v = 0.5 V/s	21	10
chemical		20	11
electrochemical		96	2
enzymatic (solution)		240	0.8
enzymatic (immobilized monolayer)		1500	"0.13"
enzymatic (immobilized multilayer) optimized number of monolayers: 4		5200	0.04

diffusion of the 2,6-DCPAPP substrate. Indeed, the fitting of the experimental data with eq 9, in which a mixed kinetic control is taken into account, is excellent.

As for enzymatic amplification, (blue dots and curves in Figure 9), the adherence to the Langmuir isotherm is even more restricted that in the preceding case. Limitation by 2,6-DCPAPP diffusion again occurs in the leveling off of the current but this is not the only factor that interferes in this concentration range. One has to take also into account that the Michaelis–Menten kinetics tends to reach saturation. All these factors had to be taken into account through the most complete eqs (12 and 2) to generate the excellent agreement observed in Figure 9. An additional factor had in fact to be considered, namely, the fact that, in the large concentration range, enzymatic amplification and direct chemical amplification by NADH are of the same order of magnitude because of Michaelis–Menten saturation of the auxiliary enzyme. The solid blue curve in Figure 9 was thus obtained by the addition of the two catalytic current densities.

2.4. Comparing the Amplification Rates, Confinement Lengths. We may now compare the different amplification strategies starting from the data gathered in Figure 10 that pertain to the system that we have taken as example. In this comparison, we focus attention on the linear response obtained, or predicted, for low values of $C^0_{N\text{-}AP}$, since it is the domain of major analytical interest.

Table 2 summarizes the amplification rates and also the confinement lengths characteristic of each method, defined as $\mu = \delta$/ampl (see section 1.5). A substantial amplification is obtained with the chemical method in our conditions (green line in Figure 10). Improvements may be sought by changing the chemical amplifier and/or its concentration. However, these changes are limited by the direct oxidation of the amplifier at the electrode surface, which rate usually parallels the rate of its reaction with the oxidized product. This is the reason that other chemical amplifiers, such as sodium borohydride, do not produce a significantly better amplification.[19] The enzymatic method, with the enzyme in solution (blue line in Figure 10), gives rise to a larger amplification. The direct oxidation of the substrate is still a limitation. The response can be improved by raising the enzyme amplifier concentration in the solution. However, the concentration of 2 μM of DI that we used in our experiments seems already a reasonable maximum. It is interesting to predict what would be the amplification rate for an immobilized monolayer of the same enzyme, using eq 18 with the parameters in Table 1 for this purpose. Amplification should then reach 1500 (cyan calibration curve in Figure 10) as in the system investigated in the preliminary note 18 where β-galactosidase was used as primary enzyme instead of alkaline phosphatase. If a thicker film could be co-immobilized with the enzyme label, we might expect an even better amplification. However as discussed in section 1.5, amplification rapidly reaches a limit (see Figure 3). In the present case, considering a surface concentration per layer of 1.5 pmol/cm^2 and a layer thickness about 0.015 μm, $C^0_{E_2} \approx 1$ mM, which corresponds to a reaction layer thickness of $\mu_F \simeq 0.04$ μm (from eq 21). Therefore, it follows that the limit is reached after the deposition of only four monolayers, leading to a predicted amplification by a factor of ca. 5000 (purple calibration curve in Figure 10).

Electrochemical amplification by means of a dual electrode system (magenta calibration curve in Figure 10) is expected to be more efficient than chemical amplification provided the gap between the two electrodes is as small as 4 μm.

As discussed in section 1.5, the confinement length for cyclic voltammetric detection is equal to the thickness of the diffusion layer, which is inversely proportional to the square root of the scan rate. At a very low scan rate, 0.01 V/s, amplification is only by a factor of 3 (red calibration curve in Figure 10) but raising the scan rate up to 0.5 V/s brings amplification (brown calibration curve in Figure 10) to a value similar to that of the chemical system. The use of higher scan rates should bring about further improvements. However a limiting factor is the fact that the definition of the peak current deteriorates simultaneously.

Concluding Remarks

In this series, dedicated to bioaffinity electrodes with in situ detection of the immobilized enzyme label product, the first part was devoted to various modes of direct electrochemical detection. In this second part, the theoretical relationships characterizing homogeneous chemical and enzymatic amplification of the primary electrochemical signal have been established. Their application to the avidin–biotin recognition in a system that involves alkaline phosphatase as enzyme label and 4-amino-2,6-dichlorophenyl phosphate as substrate, generating 4-amino-2,6-dichlorophenol as electrochemically active product, has shown an excellent agreement between theoretical predictions and experimental data. This was the case with the chemical amplification resulting from the reduction by NADH of the 2,6-dichloro-quinonimine resulting from the electrochemical oxida-

tion of 4-amino-2,6-dichlorophenol. The same is true with the more efficient amplification obtained when the reduction of 2,6-dichloro-quinonimine involves diaphorase in solution with NADH as substrate. In both cases, a detailed theoretical analysis and an independent determination of the key kinetic parameters of the system were required. This approach also allowed evidencing and optimizing the parameters that govern the amplification performances. Extension of the theoretical analysis to monolayer and multilayered films of auxiliary enzyme and to electrochemical amplification by means of closely spaced dual electrodes offered a rationale for comparing the amplification capabilities of the various possible strategies. In this connection, confinement of the profile of the product, and/or its oxidized form in the close vicinity the electrode surface appears as a key parameter of amplification.

Experimental Section

Reagents and procedures were the same as described in Part 1.[1] Lyophilised diaphorase from *Bacillus stearothermophilus* (E.C. 1.6.99.-) was purchased from Unitika (Japan) and NADH from Sigma.

An AUTOLAB potentiostat (Ecochemie) interfaced to a PC computer (GPES software) was used for cyclic voltammetry and chronoamperometry. A glassy carbon electrode (3-mm diameter) was used as working electrode. A classical water-jacketed electrochemical cell (maintained at 20 ± 0.5 °C) equipped with a saturated calomel reference electrode (SCE) and a platinum counter electrode was used. The voltammetric curves presented in this work were systematically referred to SCE.

JA7102873